Growth of Vertical Heterostructures Based on Orthorhombic SnSe/Hexagonal In$_2$Se$_3$ for High-Performance Photodetectors

Xuan-Ze Li,[a,b] Yi-Fan Wang,[a,b] Jing Xia,[*a] and Xiang-Min Meng[*a]

a. Key Laboratory of Photochemical Conversion and Optoelectronic Materials, Technical Institute of Physics and Chemistry, Chinese Academy of Sciences, Beijing, 100190, P. R. China.

b. Centre of Material Science and Optoelectronic Engineering, University of Chinese Academy of Science, Beijing, 10049, P. R. China.

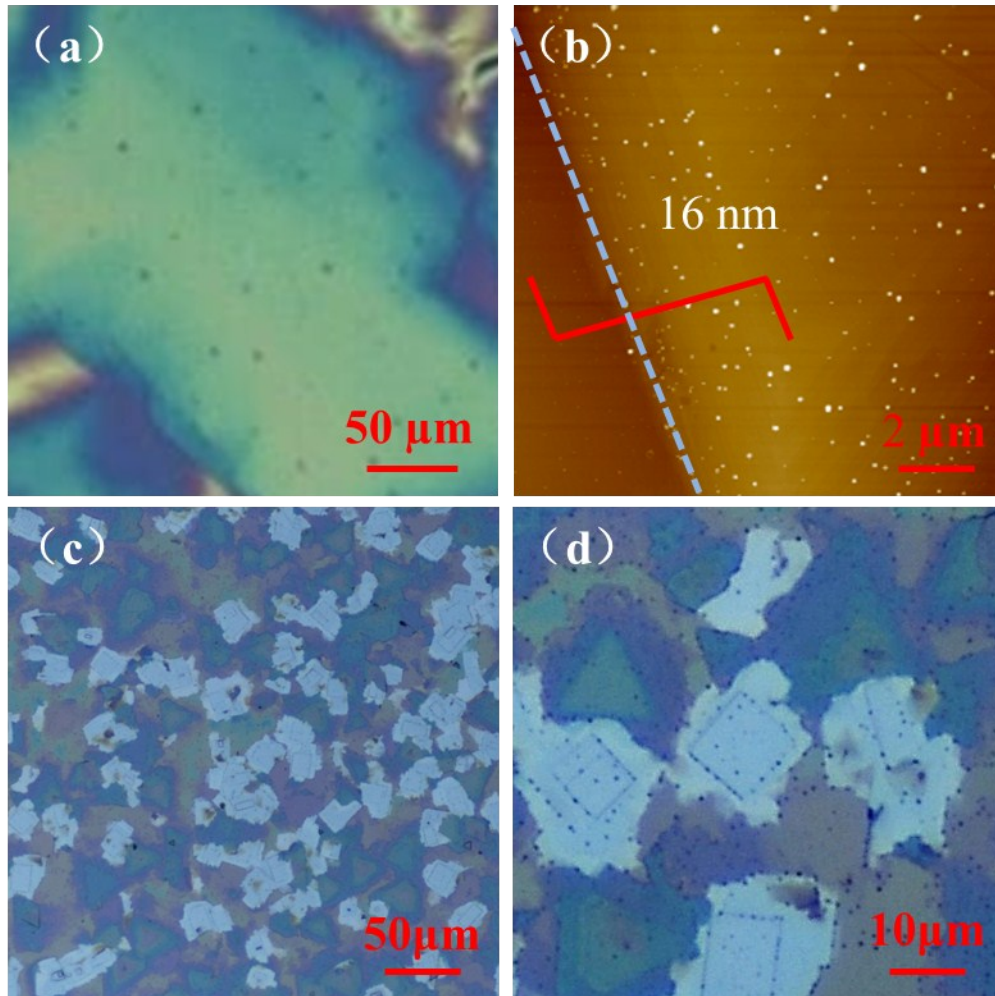E-mail: mengxiangmin@mail.ipc.ac.cn, xiajing@mail.ipc.ac.cn

Fig. S1 (a) Optical images of the In_2Se_3 sample on mica substrate. (b) AFM image and height profile of the In_2Se_3 film. (c) and (d) Optical images of the SnSe/ In_2Se_3 vertical van der waals heterostructure.
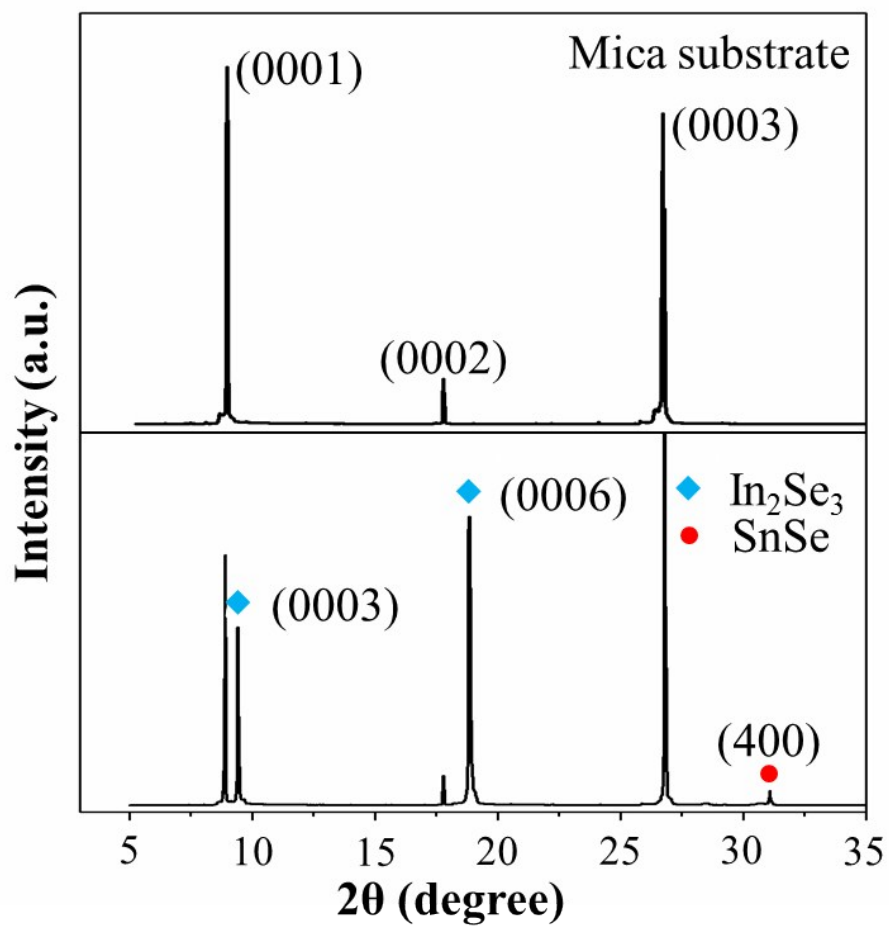
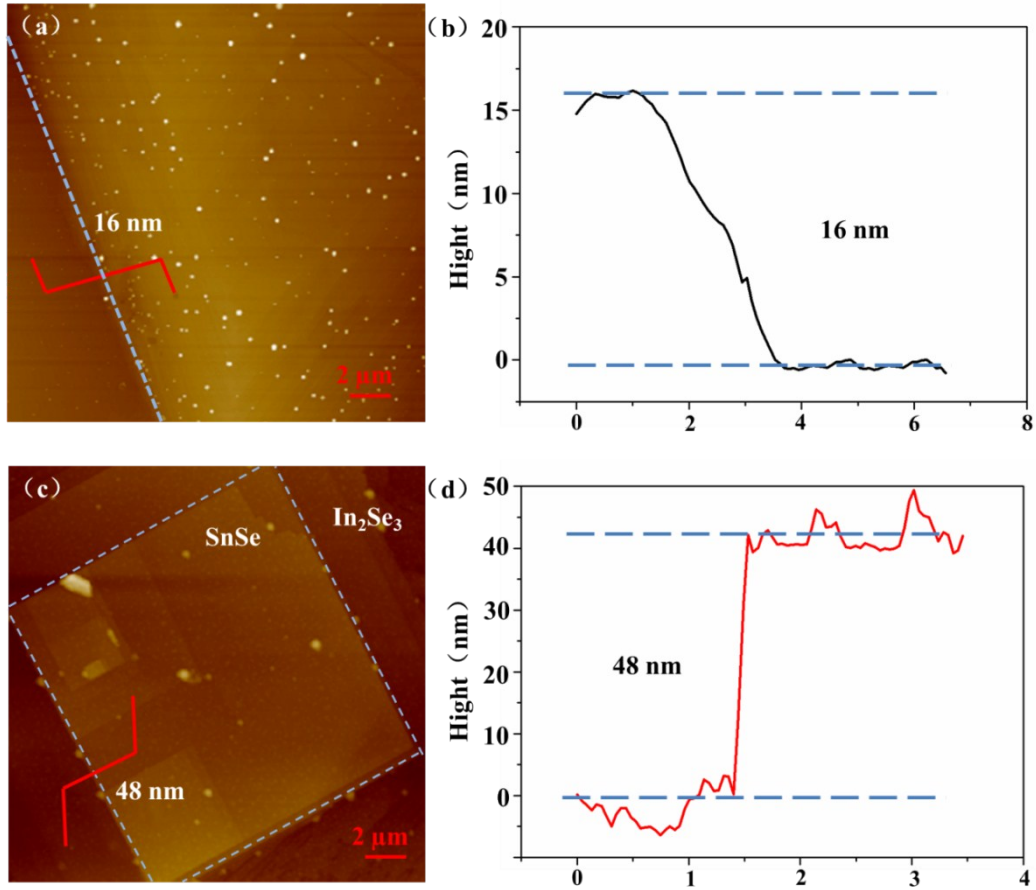**Fig S2** XRD pattern of the empty mica substrate and the as-grown SnSe/In$_2$Se$_3$.

Fig S3 (a) AFM image and height profile of the In2Se3 film. (b) Potential profile image of (a). (c) AFM image and height profile of the SnSe nanoplate. (d) Potential profile image of (c).
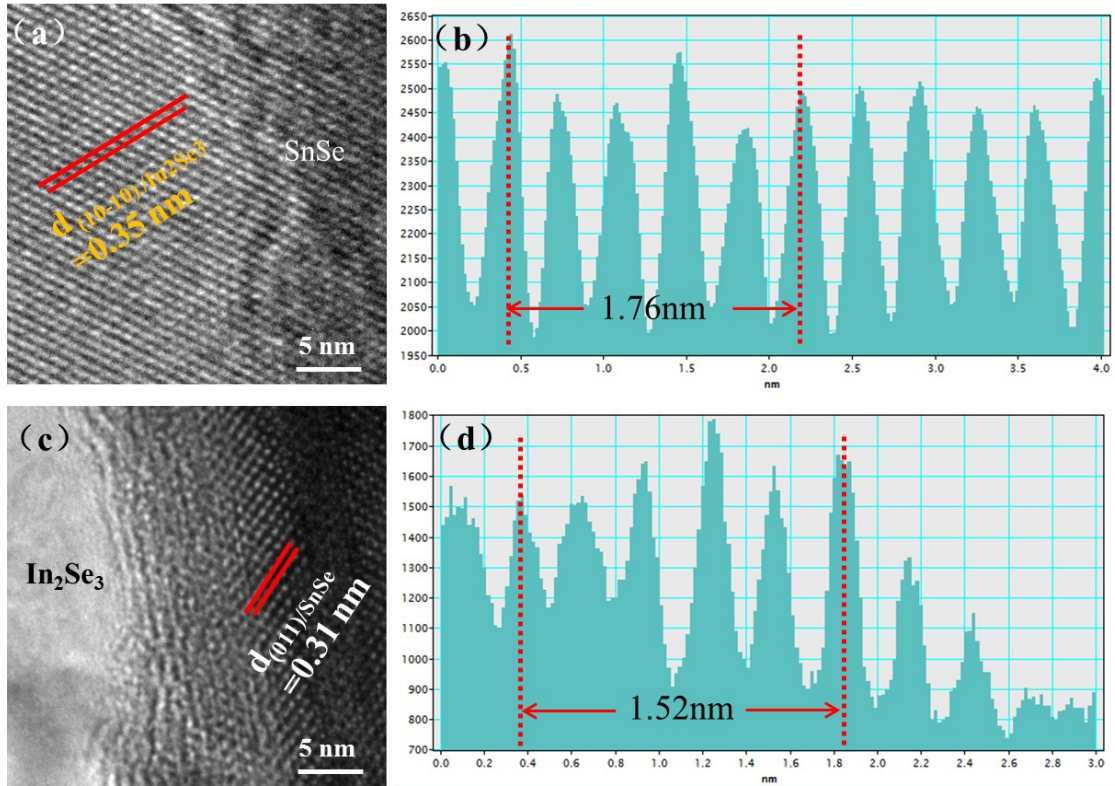
Fig S4 (a) HRTEM image of In2Se3 film in heterostructure sample (b) Pixel intensity profile of five lattice fringes. (c) HRTEM image of SnSe in heterostructure sample (b) Pixel intensity profile of five lattice fringes.
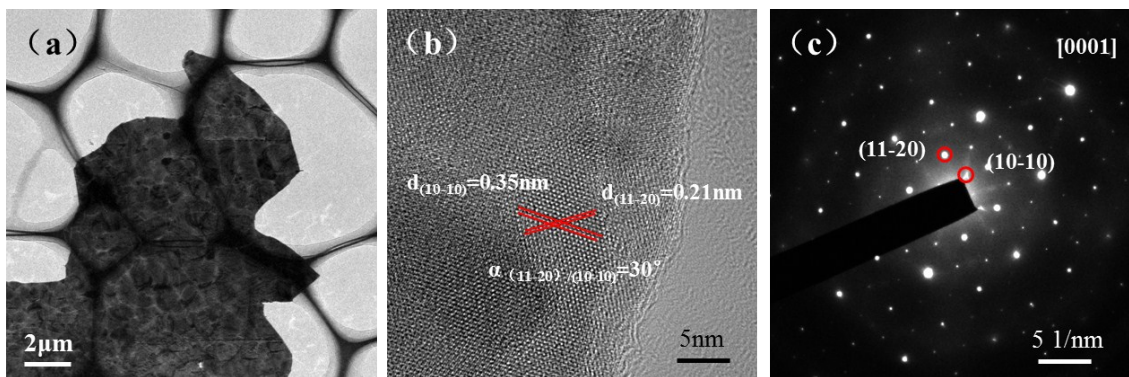
Fig. S5 (a) Bright field TEM (BFTEM) image of In_2Se_3. (b) High resolution TEM (HRTEM) image of the In_2Se_3 sample. (c) The corresponding SEAD pattern in (b).
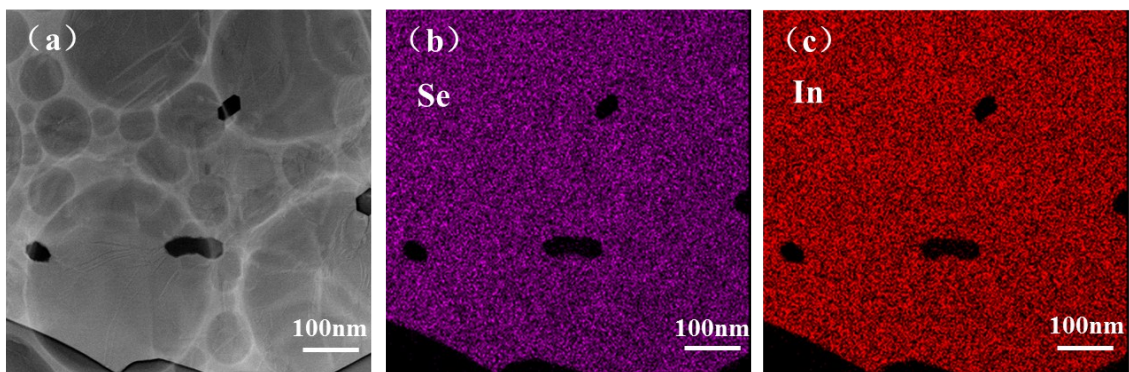

Fig. S6 (a) Dark field (DF) STEM image of In_2Se_3. (b) and (c) Elements maps of In_2Se_3 sample showing spatial distribution of Se and In.
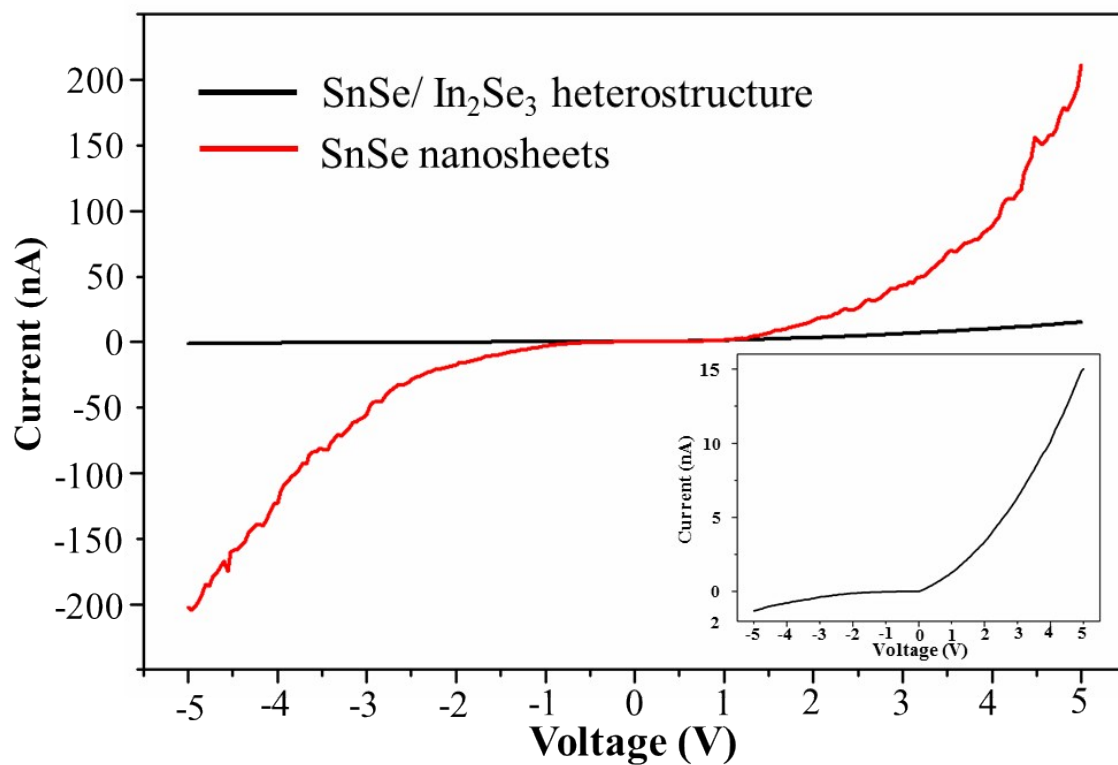
Fig. S7 *I-V* curves of the devices based on the SnSe nanosheet and SnSe/ In$_2$Se$_3$ heterostructure in the dark and the detail I-V characteristic of heterostructure shown in inserted diagram.